ORGANOMETALLICS

Article

pubs.acs.org/Organometallics

Mechanistic Insights and Implications of Dearomative Rearrangement in Copper-Free Sonogashira Cross-Coupling Catalyzed by Pd-Cy*Phine

Adrian M. Mak,*[,†] Yee Hwee Lim,*[,‡] Howard Jong,[‡] Yong Yang,[‡] Charles W. Johannes,[‡] Edward G. Robins,[§] and Michael B. Sullivan[†]

[†]Institute of High Performance Computing, 1 Fusionopolis Way, #16-16 Connexis, Singapore 138632, Singapore

[‡]Institute of Chemical and Engineering Sciences, 8 Biomedical Grove, Neuros #07-01, Singapore 138665, Singapore

[§]Singapore Bioimaging Consortium, 11 Biopolis Way, Helios #02-02, Singapore 138667, Singapore

Supporting Information

ABSTRACT: The reaction mechanism for the *in situ* prepared Pd-Cy*Phine catalyst used in copper-free Sonogashira coupling was investigated using density functional theory. In addition, the significance of the *meta*-terarylphosphine ligand architecture of Cy*Phine was probed, as it had been previously shown experimentally to augment catalytic activity relative to its biarylphosphine analogue, XPhos. The calculated reaction barriers and free energies for the steps in the catalytic cycle suggest that the suppression of a dearomative rearrangement pathway is likely to be an important feature for the improved catalytic performance observed for the Pd-Cy*Phine system.

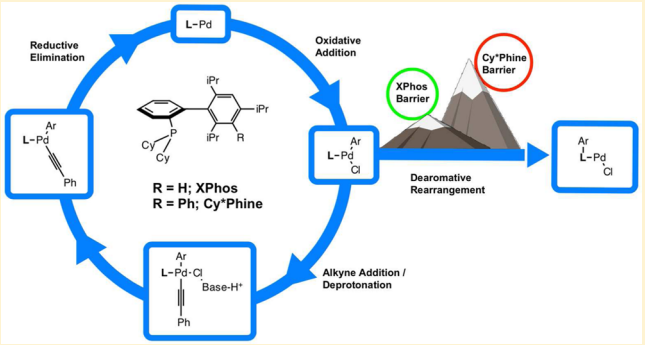

INTRODUCTION

Palladium-catalyzed Sonogashira cross-coupling is a widely used method to synthesize functional molecules containing an alkyne unit,[1−9] with applications in pharmaceuticals,[10,11] molecular wires,[12] and organic materials.[13−15] With its growing application base, a more in-depth understanding of the subtle complexities of this reaction using modern catalyst systems has also become increasingly more important. Traditional Sonogashira coupling[16] typically requires the use of a Cu(I) halide salt as a cocatalyst to have high reaction productivity. It was proposed that coordination of the alkyne to Cu(I) increases the acidity of the terminal acetylenic proton, facilitating the formation of the Cu(I) acetylide, which is used as a transmetalating agent to deliver the alkyne to the Pd that would subsequently couple the alkyne with an aryl substrate.

However, it has also been shown that, in some instances, the presence of Cu salts can have a deleterious effect on catalysis;[17−19] selected examples include participation of copper in Glaser homocoupling of two terminal alkynes to form dialkynes,[20−22] inhibition of Pd catalyst activation,[17] and oxidation of coordinatively unsaturated Pd(0) species to form halide-bridged dinuclear Pd(I) complexes that promote alkyne polymerization.[23] These resultant byproducts are wasteful and can complicate the purification of the desired compound. Thus, time-consuming method development and optimization is often necessary to yield adequate overall catalyst performance.[24] In response, the development of contemporary homogeneous Pd catalysts for the copper-free Sonogashira reaction have circumvented the drawbacks associated with the use of copper as cocatalysts.[25−39] Several notable examples for the coupling of more challenging aryl chloride substrates include contributions from Buchwald,[17,40] Beller,[41,42] Hua,[43−45] Colacot,[18,46,47] and Plenio.[5,48]

Recently, the *in situ* prepared Pd-Cy*Phine catalyst (Cy*Phine ligand depicted in Figure 1) and its $PdCl_2(Cy*Phine)_2$ precatalyst

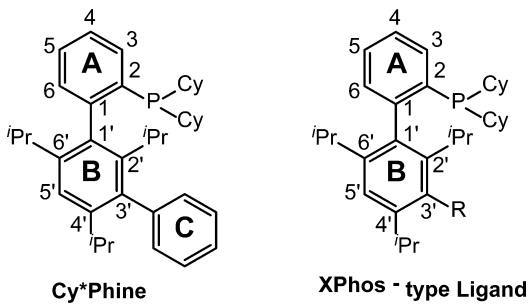

Figure 1. Cy*Phine and XPhos-type ligands (hereby labeled **L**) with the system of numbering of carbon atoms and labeling of rings used in this work. Cy = cyclohexane.

were found to promote the copper-free Sonogashira reaction with unprecedented efficiency for a broad range of challenging, electron-rich (hetero)aryl chloride substrates with high yields

Received: March 4, 2016

© XXXX American Chemical Society

DOI: 10.1021/acs.organomet.6b00186
Organometallics XXXX, XXX, XXX−XXX

and selectivity.[49,50] Similarly, the Pd-Cy*Phine catalyst system displayed greatly improved capability and scope for the Mizoroki–Heck reaction.[51] The rationale for such improved performance is still not fully understood, since the current mechanistic understanding for this class of monodentate phosphine ligands does not provide enough detail to differentiate their performance. Experimentally, the *meta*-teraryl architecture of Cy*Phine was shown to be critical to achieve ameliorated catalytic performance relative to the structurally related biarylphosphine congener XPhos. Comprehensive experimental and computational studies on Pd-catalyzed copper-free Sonogashira coupling were carried out by a number of groups[19,52−57] and summarized in recent reviews;[58,59] however, a detailed mechanism that incorporates the specific properties of bulky, multiarylated phosphine ligands still remains unclear. Starting from the general reaction cycle proposed in the literature for related Pd-centered catalysts, we employed calculations using density functional theory to gain mechanistic insight for the Pd-catalyzed copper-free Sonogashira coupling reaction, mediated by the ligands Cy*Phine and XPhos. Furthermore, other related biarylphosphine congeners with nonaryl substitutions (R = Me, OMe, F, CN) in the 3′ position (Figure 1) were also studied to better understand the structure–activity relationship of these ligand designs for Cu-free Sonogashira cross-coupling.

Previous work by Buchwald et al. had described a thermally favorable pathway by which a biarylphosphine ligand could be arylated to form a *meta*-terarylphosphine species during palladium-mediated nucleophilic fluorination.[60,61] This arylation process was shown to exist in an equilibrium (Scheme 1)

Scheme 1[a]

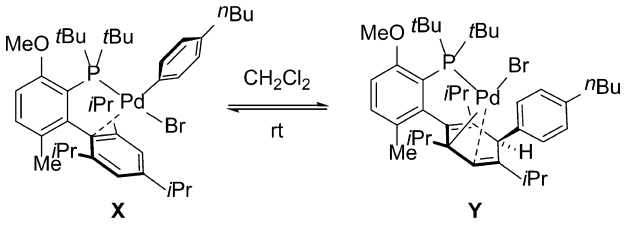

[a]X = oxidative addition product, Y = 1,2-insertion product.

with the Pd center as the mediator of a concerted 1,2-insertion of the aryl substrate into a dearomatized (second) ring of the biaryl scaffold (Figure 1, ring B). This event is hereon in referred to as dearomative rearrangement (DR). In a detailed mechanistic study of this DR phenomenon, the Buchwald group determined that the process was complex and affected by numerous factors that ranged from the substrate type to the substituents on the phosphine all playing influential roles. Nonetheless, it was proposed that the formed *meta*-terarylphosphine-palladium species was the active catalytic component. This was later affirmed as preformation of the *meta*-terarylphosphine ligand for Pd-catalyzed nucleophilic fluorination resulting in improved catalyst performance. Importantly, no further arylation was observed with the usage of the terarylphosphine ligand in their fluorination studies.

Thus, the possible modification of the biarylphosphine ligand reveals a competitive pathway to the catalytic cycle that may consume and is reactive to off-cycle events. Moreover, its dependence on the substrate's inherent characteristics may imply a potential catalytic inefficiency if the substrates are not amenable to successful arylation. Herein, we examine the impact of DR on the catalytic efficiency of the ligands of interest. We postulate that the presence of a third phenyl ring (Figure 1, ring C) of the teraryl scaffold of Cy*Phine could serve to deter the DR process, thereby removing the substrate dependence and the distraction from the catalytic cycle compared to a biarylphosphine ligand such as XPhos. Other substitutions in the 3′ position (i.e., replacement of ring C) with R = Me, CHO, CN, CF_3, NO_2, NMe_2, OMe, F, and Br were investigated computationally to determine their relative influence (sterically or electronically) on the energetics of the DR process.

THEORETICAL MODEL AND COMPUTATIONAL DETAILS

The reaction considered in this work is the previously reported copper-free Sonogashira cross-coupling of 1-*tert*-butyl-4-chlorobenzene (**S1**) and phenylacetylene (**S2**), using Cs_2CO_3 as a base, catalyzed by palladium coordinated to the Cy*Phine ligand (Scheme 2).[49]

Scheme 2. Copper-Free Sonogashira Coupling Reaction between 1-*tert*-Butyl-4-chlorobenzene and Phenylacetylene Catalyzed by Pd-Cy*Phine Catalyst

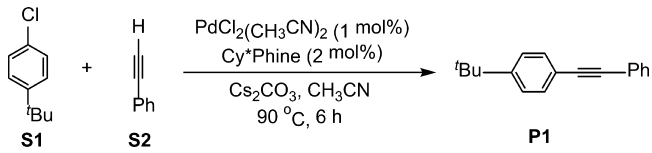

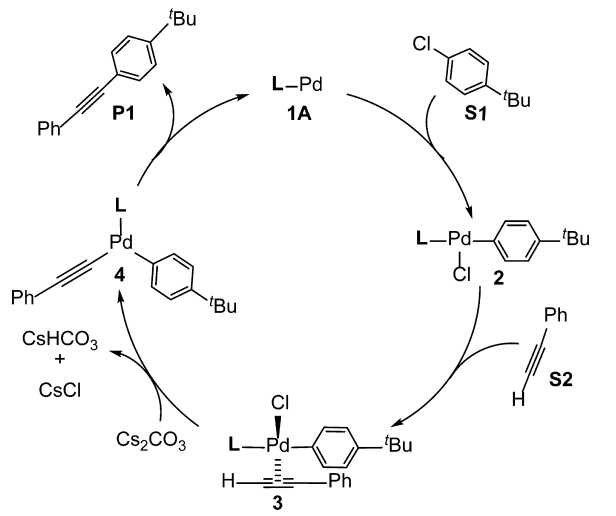

Figure 2. Generally accepted catalytic cycle for copper-free Sonogashira reaction mediated by Pd-**L**, adapted from refs 54 and 55.

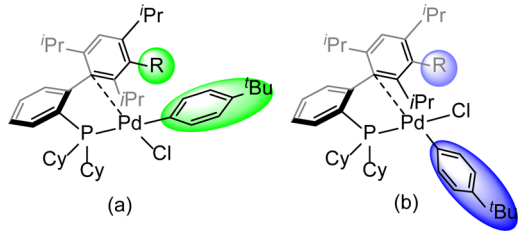

Figure 3. Illustration showing proximity of an aryl group to ring B required for its concerted insertion: (a) *cis* oxidatively added product **2**; (b) *trans* oxidatively added product **2**.

DOI: 10.1021/acs.organomet.6b00186
Organometallics XXXX, XXX, XXX–XXX

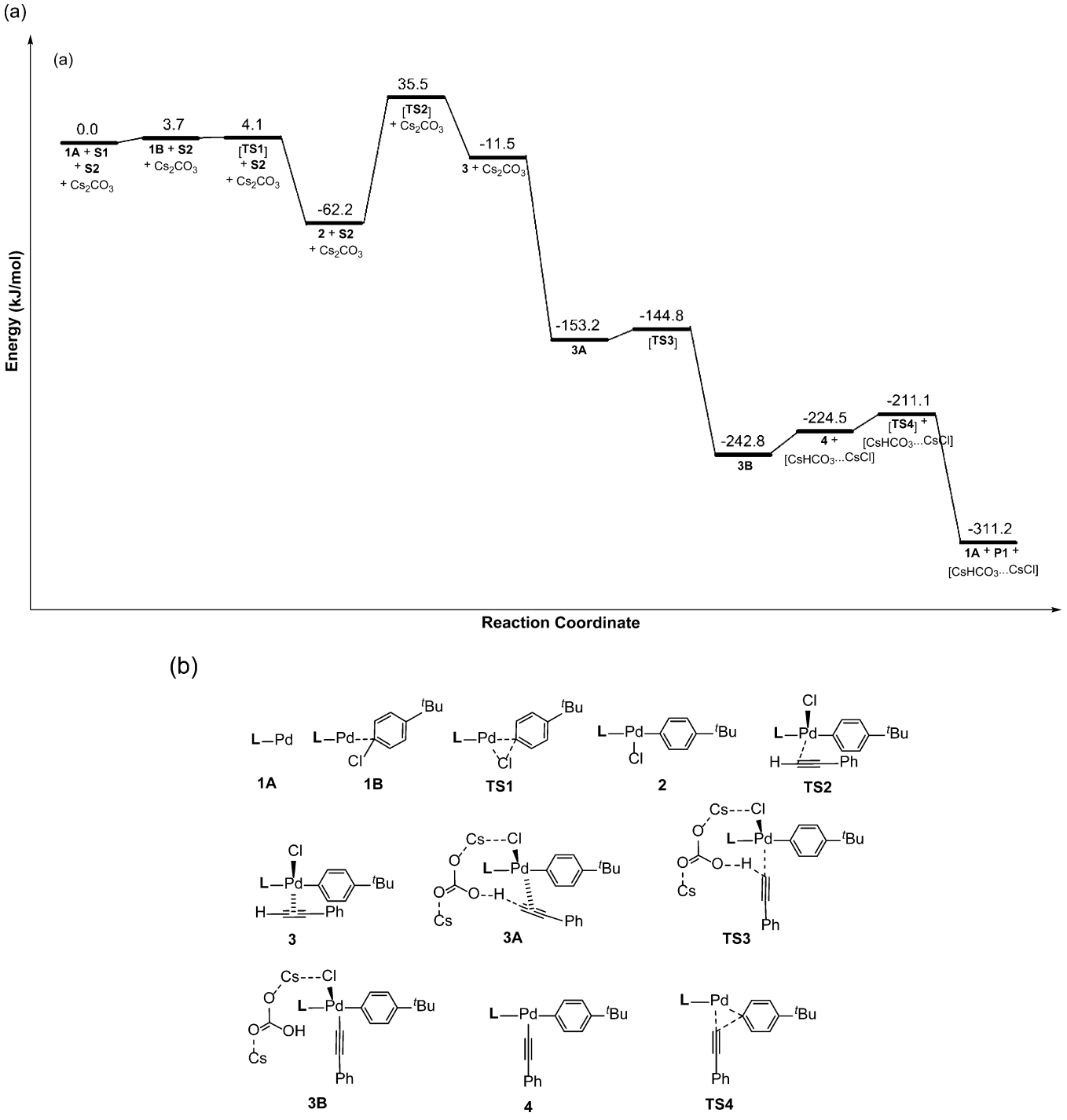

Figure 4. (a) Schematic Gibbs free energy profile (in kJ/mol) for copper-free Sonogashira coupling of **S1** and **S2**, mediated by Pd-Cy*Phine. (b) Simplified structures of species at stationary points in part (a).

An adapted version of the generally accepted mechanism of the catalytic cycle for this discussion is depicted in Figure 2.

The cycle begins with the catalytically active **1A**, a Pd(0) species stabilized by Cy*Phine (**L**), which is generated *in situ* with a precursor, $PdCl_2(CH_3CN)_2$, prior to oxidative addition (OA) of the aryl chloride **S1** to form the adduct **2**. OA of **S1** to **1A** can afford two possible conformers of the resultant complex **2** where the aryl ring in **S1** is *cis* and another where it is *trans* to ring B (see Figure 3). The *cis*−*trans* isomerization between the two conformers was determined to be an accessible process that can traverse a number of different pathways.[53] The isomerization process is understood to have a barrier of 71.1 kJ/mol for $Pd(PPh_3)_2$ and PhI as substrate,[62] and similar barriers were calculated for Pd-^{t}BuBrettPhos and 4-*n*-butylphenyl bromide as substrate.[61] Proximity of the aryl group in **S1** to ring B is required for DR to yield **D1** and **D2** (*vide infra*), and, as such, to simplify discussion, only the *cis* case is considered within the scope of this article.

Coordination of the alkyne **S2** to **2** follows, yielding an alkyne-Pd complex **3**. A number of mechanisms were proposed previously for the intermediate steps involving alkyne addition and deprotonation, from **2** to **4**. Two feasible pathways—alkyne carbopalladation[63] and alkyne deprotonation[25]—are commonly used to explain this mechanism. In light of experimental and computational evidence,[55,64] the carbopalladation cycle is assumed here to be the higher energy

DOI: 10.1021/acs.organomet.6b00186
Organometallics XXXX, XXX, XXX−XXX

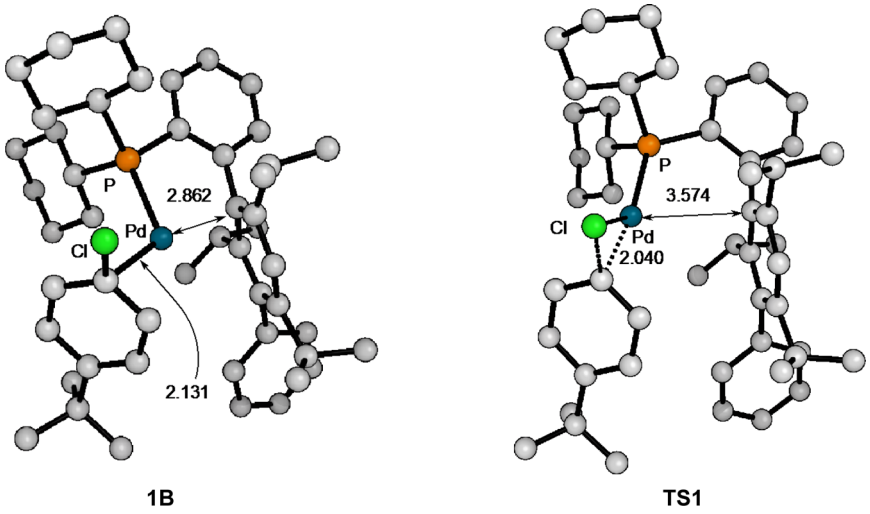

Figure 5. Optimized geometries for the adduct **1B** and the transition state for oxidative addition, **TS1**. Interatomic distances are given in angstroms. Nonessential hydrogens are removed for clarity.

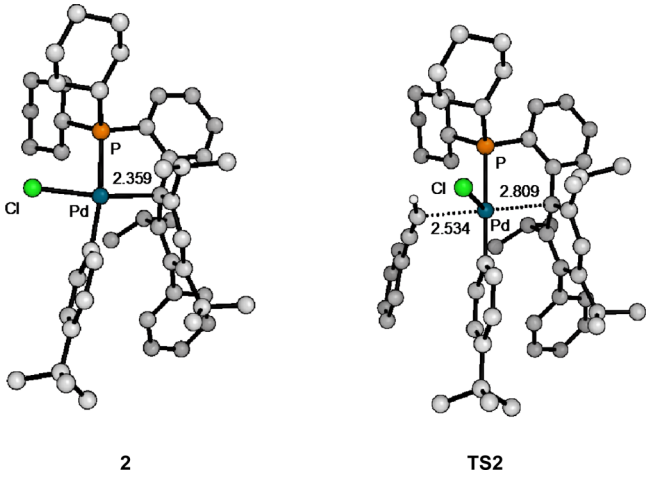

Figure 6. Optimized geometries for the oxidatively added complex **2** and the transition state for direct alkyne addition, **TS2**. Interatomic distances are given in angstroms. Nonessential hydrogens are removed for clarity.

pathway and contributes less to the overall yield of the product. The theoretical model and further discussions are thus based on the premises adopted in the alkyne deprotonation pathway. Of the two deprotonation-type mechanisms, it was rationalized by Nájera, Lledós, and Ujaque et al.[55] that the cationic mechanism is favored for phenylacetylenes with highly electron donating groups (EDGs) as substituents, while the anionic mechanism is favored for phenylacetylenes with moderate EDGs and electron withdrawing groups (EWGs) and unsubstituted phenylacetylene. Thus, it is reasonable to expect that the lower energy catalytic cycle for our choice of substrates follows the anionic route. In any case, the alkyne-Pd complex **3** is deprotonated to yield the Pd-alkynylide complex **4**. The tolane product **P1** is reductively eliminated to regenerate the active catalyst **1**, and the cycle is thus completed.

In our calculations, the PBE density functional of Perdew, Burke, and Ernzerhof[65] was used, with the LANL2DZ basis set for all atoms and associated pseudopotentials for Pd and Cs,[66−68] as implemented in a development version of Q-Chem.[69] The choice of density functional and basis set is guided by prior work from Buchwald et al.,[61] had good agreement of PBE/LANL2DZ geometries of *trans*-Pd-XPhos with solid-state structures, and was also chosen for its reproduction of experimental free energies for oxidative addition of *para*-substituted phenyl bromides. Harmonic frequency calculations were carried out to ensure the nature of the local minima and transition states, which were also used in the estimation of Gibbs free energies at 298 K and 1 atm for all species identified in the catalytic cycle. Intrinsic reaction coordinate (IRC)[70] calculations were also carried out for the transition states to verify that they connect reactants to products.

RESULTS AND DISCUSSION

I. Oxidative Addition, Alkyne Addition and Deprotonation, and Reductive Elimination. The calculated Gibbs free energy profile for the copper-free Sonogashira coupling of 1-*tert*-butyl-4-chlorobenzene **S1** and phenylacetylene **S2** mediated by Pd-Cy*Phine is depicted in Figure 4.

The oxidative addition of aryl halides to phosphine-ligated palladium has been well explored,[71−73] and the trend of aryl halide reactivity was established to increase in the order ArF < ArCl < ArBr < ArI.[74] In the case of Cy*Phine (R = Ph) the OA step yielding *cis*-OA product **2** is exergonic by 62.2 kJ/mol, with an unexpected low barrier of 4.0 kJ/mol with respect to the reactants. The possibility of forming a prereaction adduct between **1A** and **S1** was explored, and a local minimum, **1B**, was located −73.4 kJ/mol with respect to the reactants on the zero point energy (ZPE) corrected potential energy surface. However, upon introducing thermal and free energy corrections, the adduct is 0.4 kJ/mol higher in energy with respect to **1A** + **S1**. Similar to the systems explored by Vikse et al., the Pd center in **1B** interacts with the phenyl ring in **S1**.[73] It was observed that the Pd···C1′ distance in ring B increases from **1A** to **1B**, from 2.264 Å to 2.862 Å, eventually being 3.574 Å at the OA transition state **TS1**, with P, Pd, Cl, and the phenyl carbon in **S1** adopting trigonal planar geometry (Figure 5).

Following the deprotonation-type mechanism,[25] the next step involves the addition of the alkyne to **2**. The barrier of 97.8 kJ/mol is comparatively much larger than the OA step, and the reaction is endergonic by 50.8 kJ/mol, as square planar coordination geometry about the Pd center is disrupted to accommodate five ligands (Figure 6, **TS2**). Subsequently, the Pd again becomes unbound to carbon 1′ in ring B, with the Pd···C1′ distance in **3** at 4.039 Å. Coordination of Cs_2CO_3 to the alkyne to form **3A** is exergonic by 141.7 kJ/mol, possibly due to the formation of the Cs···Cl interaction.

The optimized geometries for the local minima and transition states involved in the deprotonation step are depicted in Figure 7. Deprotonation of the Pd-attached alkyne in **3A**

DOI: 10.1021/acs.organomet.6b00186
Organometallics XXXX, XXX, XXX−XXX

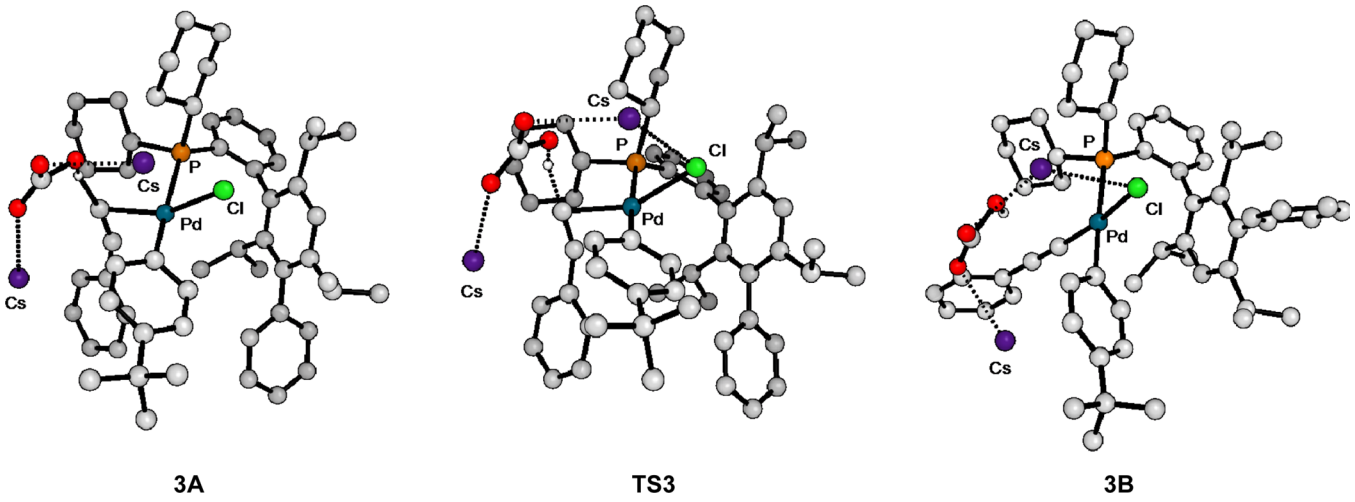

Figure 7. Optimized geometries for Cs_2CO_3-coordinated complex **3A**, transition state for deprotonation **TS3**, and postdeprotonation complex **3B**. Nonessential hydrogens are removed for clarity.

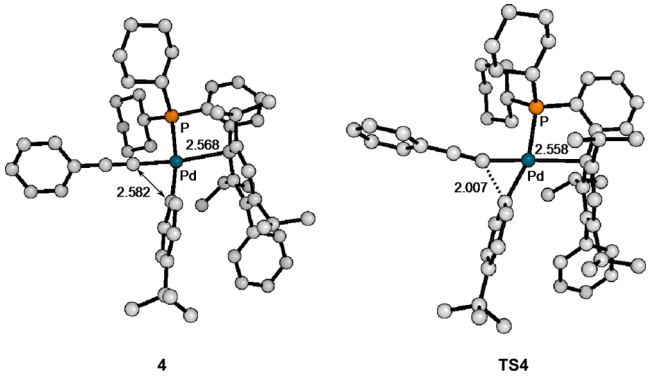

Figure 8. Optimized geometries for the complex **4** and the transition state for reductive elimination, **TS4**. Interatomic distances are given in angstroms. Nonessential hydrogens are removed for clarity.

to yield **3B** is exergonic as the alkyne rearranges from a Dewar−Chatt−Duncanson π-type donor to σ-donor and π^*-acceptor as an alkynylide.[75] The barrier for deprotonation by Cs_2CO_3 is 8.4 kJ/mol. Deprotonation products $CsHCO_3$ and CsCl are complexed in the structure of **3B**. Dissociation of this [$CsHCO_3$···CsCl] complex yields **4**, with the Pd···C1′ bond reengaged with a bond distance of 2.558 Å. Subsequently, reductive elimination (RE) of the product **P1** occurs with a small barrier of 13.4 kJ/mol and is exergonic by 86.6 kJ/mol, after which the catalytically active **1A** is regenerated. Optimized geometries for the local minimum **4** and the transition state for RE, **TS4**, are depicted in Figure 8.

The energy barriers and reaction free energies for the species in the putative catalytic route (oxidative addition → alkyne addition → deprotonation → reductive elimination) mediated by Pd-Cy*Phine and Pd-XPhos are summarized in Table 1. Barriers for OA were calculated from the Gibbs free energy difference between the OA transition state and **1A** + **S1** or the pre-OA adduct **1B**, whichever is lower. Following this method, Cy*Phine yields the lowest barrier for the OA process for the systems that were studied. The rapid formation of **2** is conducive for the progress of cross-coupling and is possibly related to increased rate of formation of the cross-coupled product **P1** in previous experimental studies.[49,50]

The highest barrier for the catalytic cycle is the alkyne addition step, thus making it the rate-limiting step in the

Table 1. Reaction Barriers $\Delta G^{\ddagger}$ and Free Energies ΔG in kJ/mol, at 298 K and 1 atm, for Oxidative Addition, Alkyne Addition, and Reductive Elimination Steps in the Catalytic Cycle

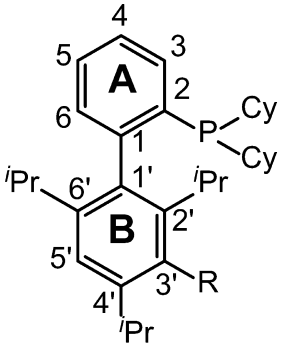

XPhos - type Ligand

	3′ substituent, R					
	Ph	H	Me	OMe	F	CN
Oxidative Addition						
barrier	4.0[a]	23.2[b]	26.5[b]	10.4[a]	14.1[b]	13.6[a]
reaction free energy	−62.3	−45.8	−74.1	−48.3	−62.7	−57.1
Alkyne Addition						
barrier	97.8	69.6	71.1	85.8	96.3	78.7
reaction free energy	50.8	29.4	45.8	33.0	40.9	32.8
Deprotonation						
barrier	8.4	5.2	5.5	7.8	1.6	1.0
reaction free energy	−89.6	−111.1	−101.6	−103.4	−93.9	−106.0
Reductive Elimination						
barrier	13.4	15.8	7.3	7.1	17.4	9.0
reaction free energy	−86.6	−88.2	−73.2	−111.1	−74.9	−84.3

[a]ΔG(TS − (reactants **1A** + **S1**)). [b]ΔG(TS − adduct **1B**).

putative pathway. The alkyne addition barrier for Cy*Phine is the highest at 97.8 kJ/mol compared to 69.6 kJ/mol for XPhos. These results are counterintuitive, as the experimental formation of **P1** catalyzed by Pd-Cy*Phine is rapid in the first 2 h, while that catalyzed by Pd-XPhos shows a lower rate.[49]

In order to gain insight on the effects of other substituents on the 3′ position of ring B in the ligand, the free energy profile of

DOI: 10.1021/acs.organomet.6b00186
Organometallics XXXX, XXX, XXX−XXX

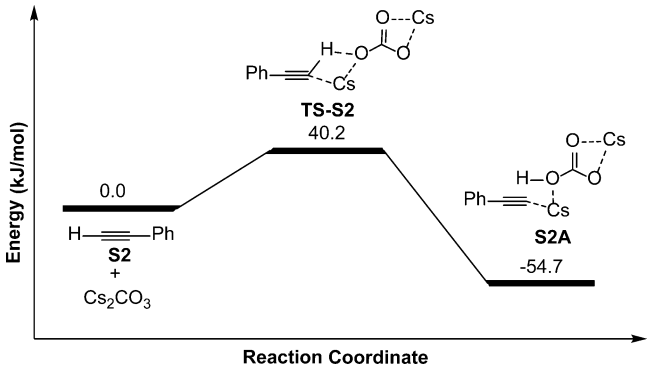

Figure 9. Schematic free energy profile of reaction of phenylacetylene **S2** with Cs_2CO_3.

the putative catalytic route was also computed and traced for selected congeners of Cy*Phine, namely, for R = Me, OMe, F, and CN (Figure 1). These corresponding free energy profiles are provided in the Supporting Information. Similar trends were observed, with the highest barrier in the catalytic pathway being the alkyne addition step and all of which are higher than that for XPhos. Taken together, this suggests that there could be an alternative lower energy pathway that is being followed by Pd-Cy*Phine or the existence of processes external to the main catalytic pathway that are beneficial to ligands that are substituted in their 3′ position.

II. Role of the Cs_2CO_3 Base. In an attempt to explain the rapid formation of **P1** in the first 2 h for the Pd-Cy*Phine-catalyzed reaction compared to that catalyzed by Pd-XPhos,

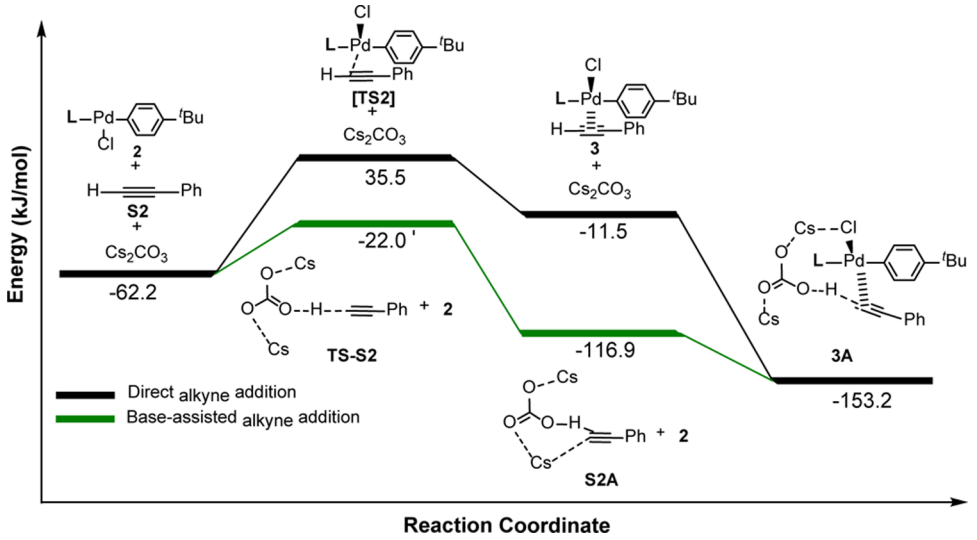

Figure 10. Schematic potential energy surface of **2** + **S2** + Cs_2CO_3 to **3A** subsection from Figure 5a above, showing pathway involving direct alkyne addition and the more favorable Cs_2CO_3-assisted alkyne addition via the formation of **S2A**.

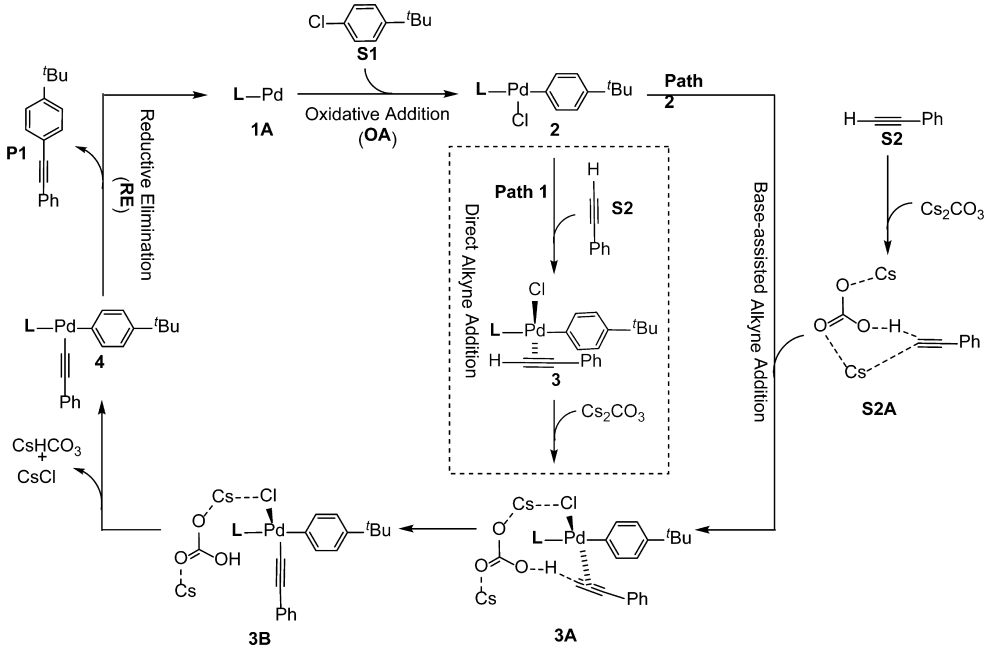

Figure 11. Proposed revised mechanism for copper-free Sonogashira coupling with Cs_2CO_3 as base.

DOI: 10.1021/acs.organomet.6b00186
Organometallics XXXX, XXX, XXX−XXX

we explored the role of the Cs_2CO_3 base in this reaction. Base screening results using $PdCl_2(CH_3CN)_2$ precursor and acetonitrile as a solvent showed lower yields associated with amine bases (12% with Et_3N, 23% with piperidine) and Na_2CO_3 (30%), but improved yields with the stronger bases K_2CO_3 (67%) and Cs_2CO_3 (91%).[49] The alkynylic proton has a pK_a of 28.8 in DMSO,[76] and the bare alkyne would be susceptible to react with the excess base in the reaction mixture. Also, the reaction is usually carried out in the presence of excess amounts of base, and as such, we considered a possible external reaction of the alkyne with Cs_2CO_3.

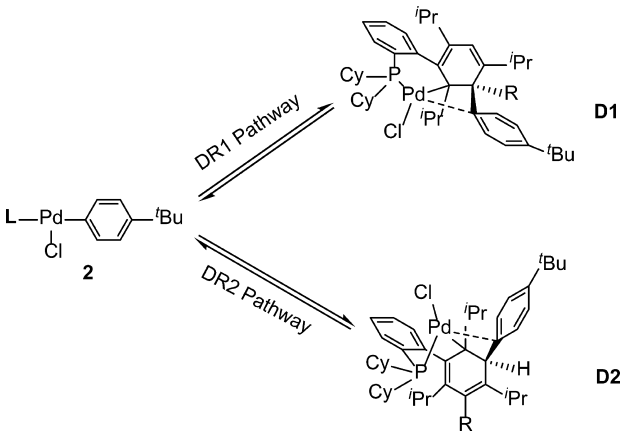

Figure 12. Dearomative rearrangement (DR) pathways available for oxidatively added complex **2**.

Cs_2CO_3 was found in other studies to promote the reactions of terminal alkynes in several cases in the absence of Cu(I) and Pd, for instance, in reactions with pyrrolidone,[77] iodine,[78] and carbon dioxide.[79] CsF is also known to act as a base to yield cesium alkynylides in some cases.[80] In this case, the reaction between Cs_2CO_3 with **S2** was found to be exergonic by 54.7 kJ/mol, with a reaction barrier of 40.2 kJ/mol. The schematic free energy profile corresponding to this process is depicted in Figure 10. The formation of the complex **S2A** competes with coordination of **S2** to the Pd center in **2** and is independent of the amount of **2** in the reaction mixture. Here, the base acts in a manner similar to transmetalation by Cu(I)

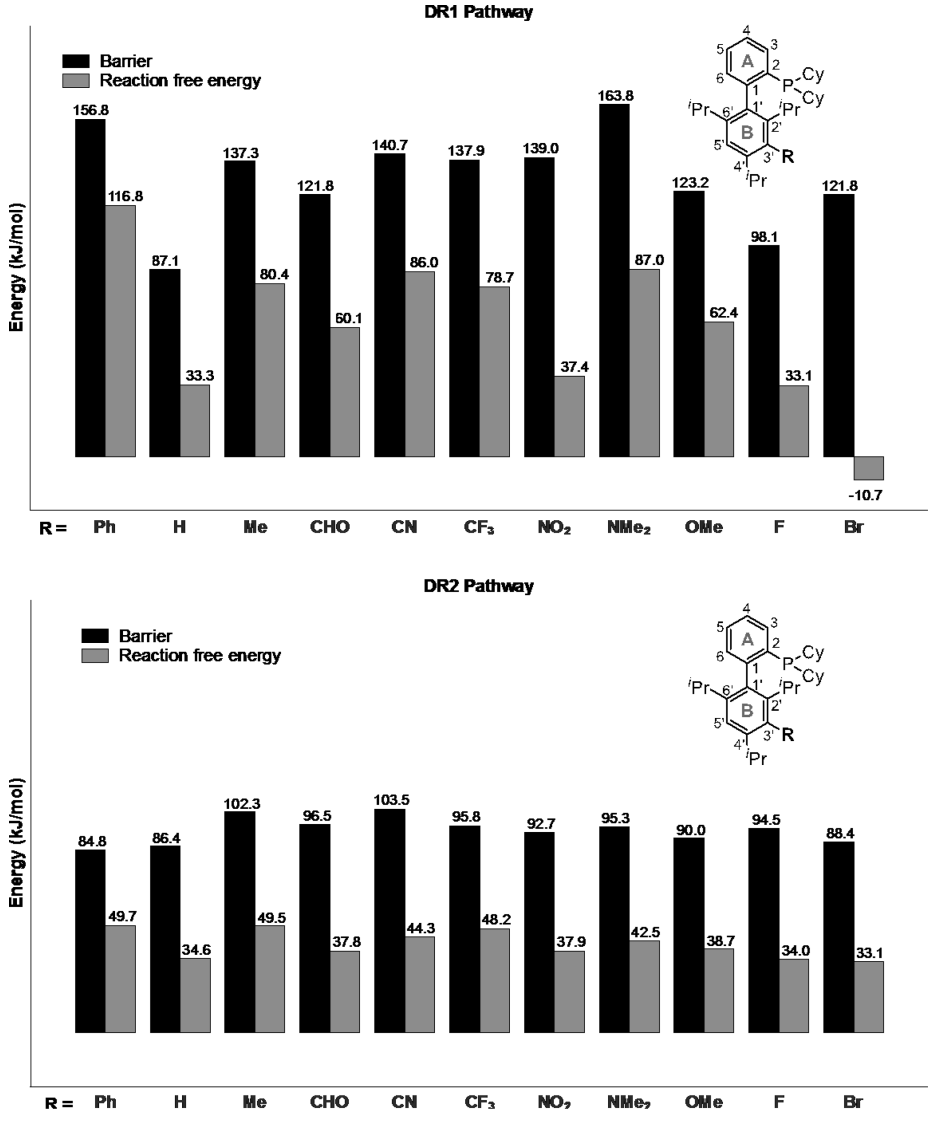

Figure 13. Variation of the Gibbs free energy barrier and free energy of reaction at 298 K ($\Delta G^{\ddagger}_{298}$ and ΔG_{298}) in both dearomative rearrangement pathways for various substituents R.

DOI: 10.1021/acs.organomet.6b00186
Organometallics XXXX, XXX, XXX−XXX

cocatalysts, delivering the alkyne to Pd, which would then facilitate its coupling to the other aryl group.

A subsection of the schematic potential energy surface in Figure 4a and the schematic potential energy surface of direct reaction of Cs_2CO_3 and the alkyne **S2** from Figure 9 are depicted together in Figure 10. This illustrates that the alternate route involving Cs_2CO_3-assisted alkyne addition could be a viable and competitive pathway to that outlined in Figure 2. A revised catalytic cycle that illustrates this is shown in Figure 11. Along with other barriers calculated in the catalytic cycle, this lower barrier Cs_2CO_3-assisted pathway may provide a partial explanation for the high initial rate for the Pd-Cy*Phine catalyst. However, it should be noted that this lower barrier pathway is likely to be operating for XPhos as well.

Despite the existence of a competing, energetically favorable pathway for the rate-determining alkyne addition step, the energetics do not provide sufficient evidence to rationalize a large difference in performance between Cy*Phine and XPhos. External factors outside the main catalytic cycle must be contributing to elevate the catalytic activity for Cy*Phine. We next examine the mechanism of the dearomative rearrangement and its influence on catalysis using the ligands of interest.

III. Dearomative Rearrangement. The *cis*-oxidatively added complex **2** can undergo DR, where the aryl group in **S1** inserts into ring B. As shown in Figure 12, there are two possible DR routes for complex **2**, one involving the insertion of the *tert*-butylphenyl group to the 3′ position of ring B (DR1) and the other involving insertion to the 5′ position (DR2).

Reaction barriers and free energies of DR1 and DR2 were calculated for Cy*Phine and various biarylphosphine analogues, R = H (XPhos), Me, CHO, CN, CF_3, NO_2, NMe_2, OMe, F, and Br (Figure 13). In all cases examined except R = Br, the DR1 pathway is endergonic. The lowest barrier for DR1 is that for R = H (87.1 kJ/mol), which becomes the baseline reference if substituent size is the primary consideration in correlating DR1 barriers with the ease of the DR process. Thus, all investigated non-hydrogen substitutions in the 3′ position of ring B present a higher barrier to DR1, with the most notable being the more sterically encumbered substitutions, R = Ph and NMe_2, having barriers of 156.8 and 163.8 kJ/mol, respectively.

As all of the ligands are unsubstituted in the 5′ ring position, the DR2 channel was also observed to be somewhat independent of the choice of substituents on the 3′ carbon. Calculated barriers were also prohibitively high, ranging from 86 kJ/mol for R = H to 103.5 kJ/mol for R = CN, and free energies of reaction were positive, ranging from 33.1 kJ/mol for R = Br to 49.7 kJ/mol for R = Ph. Although a DR2 insertion product has not been detected or isolated, calculations show that it is possible to form and can eventually rearrange to a 1,4-insertion product via a 1,3-allylic shift of the Pd center on ring B.[61]

The large difference in the DR energetics for Pd-Cy*Phine and Pd-XPhos compared to the steps in the main catalytic cycle suggests that the hindrance of the DR pathway is likely a main contributor to the enhanced catalytic performance exhibited by Pd-Cy*Phine. Moreover, larger R substituents such as Ph (Cy*Phine) and NMe_2 have higher barriers for DR1, suggesting a correlation likely exists with increasing substituent size. The highly positive free energy (ΔG) of the DR1 reaction for Pd-Cy*Phine also indicates the chemical equilibrium position lies on the side of the reactants (i.e., the post-OA complex **2**). This avails of **2** to proceed along the catalytic cycle, preserving the active species in its unaltered form, thus yielding more desired product than a nonsubstituted counterpart.

An auxiliary observation for alternative ligand design could be discerned from this theoretical calculation. However, further experimental evidence is necessary to corroborate the computational results, which are currently being explored in our laboratories and will be reported in due course.

CONCLUSIONS

The mode of action of Pd-Cy*Phine in the copper-free Sonogashira cross-coupling of *p-tert*-butylphenyl chloride and phenylacetylene was characterized using first-principles calculations based on density functional theory. Oxidative addition and reductive elimination steps mostly involve low reaction barriers and are exergonic. The rate-limiting step involves the addition of the isolated alkyne to the Pd center and its deprotonation, which is prohibitively high for Cy*Phine to rationalize the rapid initial kinetics of the catalytic reaction.

A plausible alternative pathway for alkyne addition to Pd involving the prior formation of the $CsHCO_3$-alkynylide ion pair was considered The barriers for Cs_2CO_3-assisted addition are lower than that for the direct addition of an isolated alkyne, thus rendering the Cs_2CO_3-assisted alkyne addition as the preferred rate-limiting step. Similar reaction barriers and free energies for the steps in the catalytic cycle were also found for a series of biarylphosphine analogues including XPhos.

However, unproductive off-cycle events such as the dearomative rearrangement pathways are highly dependent on ligand architecture. High barriers and endergonic free energies from non-hydrogen substitutions at the 3′ position of the ligand backbone suggest that these systems have a lower likelihood of dearomative rearrangement pathways interfering with catalysis. Barrier heights for DR appear to correlate with substituent size on the insertion site. The stark differences in the ΔG and $\Delta G^{\ddagger}$ of the DR processes examined implicate that substitutions in the 3′ position (as in Cy*Phine with R = Ph) serve to block DR channels that deviate from productive catalysis. This is in good agreement with the improved catalytic performance observed between Cy*Phine and XPhos in Pd-catalyzed copper-free Sonogashira cross-coupling.

ASSOCIATED CONTENT

Supporting Information

The Supporting Information is available free of charge on the ACS Publications website at DOI: 10.1021/acs.organomet.6b00186.

Free energy profiles (PDF)
Atomic coordinates of optimized structures (XYZ)

AUTHOR INFORMATION

Corresponding Authors

*E-mail (A. M. Mak): makwk@ihpc.a-star.edu.sg.
*E-mail (Y. H. Lim): lim_yee_hwee@ices.a-star.edu.sg.

Notes

The authors declare no competing financial interest.

ACKNOWLEDGMENTS

Financial support for this work was provided by the A*STAR Joint Council Office (JCO), the Singapore 1st JCO Developmental Programme (DP) (grant JCO 1230400020), the A*STAR Institute of High Performance Computing (IHPC), A*STAR Institute of Chemical and Engineering Sciences (ICES), and the A*STAR Singapore Bioimaging

DOI: 10.1021/acs.organomet.6b00186
Organometallics XXXX, XXX, XXX−XXX

Consortium (SBIC). This work was supported by the A*STAR Computational Resource Centre (A*CRC) through the use of its high-performance computing facilities.

REFERENCES

(1) Tykwinski, R. R. *Angew. Chem., Int. Ed.* **2003**, *42* (14), 1566−1568.
(2) Chinchilla, R.; Nájera, C. *Chem. Rev.* **2007**, *107* (3), 874−922.
(3) Doucet, H.; Hierso, J.-C. *Angew. Chem., Int. Ed.* **2007**, *46* (6), 834−871.
(4) Plenio, H. *Angew. Chem., Int. Ed.* **2008**, *47* (37), 6954−6956.
(5) Fleckenstein, C. A.; Plenio, H. *Chem. Soc. Rev.* **2010**, *39* (2), 694−711.
(6) Jenny, N. M.; Mayor, M.; Eaton, T. R. *Eur. J. Org. Chem.* **2011**, *2011* (26), 4965−4983.
(7) Chinchilla, R.; Nájera, C. *Chem. Soc. Rev.* **2011**, *40* (10), 5084.
(8) Johansson Seechurn, C. C. C.; Kitching, M. O.; Colacot, T. J.; Snieckus, V. *Angew. Chem., Int. Ed.* **2012**, *51* (21), 5062−5085.
(9) Hierso, J.-C.; Beaupérin, M.; Saleh, S.; Job, A.; Andrieu, J.; Picquet, M. *C. R. Chim.* **2013**, *16* (6), 580−596.
(10) Beutler, U.; Mazacek, J.; Penn, G.; Schenkel, B.; Wasmuth, D. *Chim. Int. J. Chem.* **1996**, *50* (4), 154−156.
(11) Frigoli, S.; Fuganti, C.; Malpezzi, L.; Serra, S. *Org. Process Res. Dev.* **2005**, *9* (5), 646−650.
(12) Hortholary, C.; Coudret, C. *J. Org. Chem.* **2003**, *68* (6), 2167−2174.
(13) Trilla, M.; Pleixats, R.; Man, M. W. C.; Bied, C.; Moreau, J. J. E. *Adv. Synth. Catal.* **2008**, *350* (4), 577−590.
(14) Raimundo, J.-M.; Lecomte, S.; Edelmann, M. J.; Concilio, S.; Biaggio, I.; Bosshard, C.; Günter, P.; Diederich, F. *J. Mater. Chem.* **2004**, *14* (3), 292.
(15) Schiedel, M.-S.; Briehn, C. A.; Bäuerle, P. *J. Organomet. Chem.* **2002**, *653* (1−2), 200−208.
(16) Dasaradhan, C.; Kumar, Y. S.; Prabakaran, K.; Khan, F.-R. N.; Jeong, E. D.; Chung, E. H. *Tetrahedron Lett.* **2015**, *56* (6), 784−788.
(17) Gelman, D.; Buchwald, S. L. *Angew. Chem., Int. Ed.* **2003**, *42* (48), 5993−5996.
(18) Pu, X.; Li, H.; Colacot, T. J. *J. Org. Chem.* **2013**, *78* (2), 568−581.
(19) Ljungdahl, T.; Pettersson, K.; Albinsson, B.; Mårtensson, J. *J. Org. Chem.* **2006**, *71* (4), 1677−1687.
(20) Glaser, C. *Ber. Dtsch. Chem. Ges.* **1869**, *2* (1), 422−424.
(21) Glaser, C. *Ann. Chem. Pharm.* **1870**, *154* (2), 137−171.
(22) Jover, J.; Spuhler, P.; Zhao, L.; McArdle, C.; Maseras, F. *Catal. Sci. Technol.* **2014**, *4* (12), 4200−4209.
(23) Aufiero, M.; Proutiere, F.; Schoenebeck, F. *Angew. Chem., Int. Ed.* **2012**, *51* (29), 7226−7230.
(24) Bandini, M.; Luque, R.; Budarin, V.; Macquarrie, D. J. *Tetrahedron* **2005**, *61* (41), 9860−9868.
(25) Soheili, A.; Albaneze-Walker, J.; Murry, J. A.; Dormer, P. G.; Hughes, D. L. *Org. Lett.* **2003**, *5* (22), 4191−4194.
(26) Allouch, F.; Vologdin, N. V.; Cattey, H.; Pirio, N.; Naoufal, D.; Kanj, A.; Smaliy, R. V.; Savateev, A.; Marchenko, A.; Hurieva, A.; Koidan, H.; Kostyuk, A. N.; Hierso, J.-C. *J. Organomet. Chem.* **2013**, *735*, 38−46.
(27) Firouzabadi, H.; Iranpoor, N.; Gholinejad, M. *J. Mol. Catal. A: Chem.* **2010**, *321* (1−2), 110−116.
(28) Huang, H.; Liu, H.; Jiang, H.; Chen, K. *J. Org. Chem.* **2008**, *73* (15), 6037−6040.
(29) Buxaderas, E.; Alonso, D. A.; Nájera, C. *Eur. J. Org. Chem.* **2013**, *2013* (26), 5864−5870.
(30) Lee, D.-H.; Kwon, Y.-J.; Jin, M.-J. *Adv. Synth. Catal.* **2011**, *353* (17), 3090−3094.
(31) Sabounchei, S. J.; Ahmadi, M.; Nasri, Z.; Shams, E.; Panahimehr, M. *Tetrahedron Lett.* **2013**, *54* (35), 4656−4660.
(32) Ruiz, J.; Cutillas, N.; López, F.; López, G.; Bautista, D. *Organometallics* **2006**, *25* (24), 5768−5773.
(33) Yang, F.; Cui, X.; Li, Y.; Zhang, J.; Ren, G.; Wu, Y. *Tetrahedron* **2007**, *63* (9), 1963−1969.
(34) Böhm, V. P. W.; Herrmann, W. A. *Eur. J. Org. Chem.* **2000**, *2000* (22), 3679−3681.
(35) Saleh, S.; Picquet, M.; Meunier, P.; Hierso, J.-C. *Tetrahedron* **2009**, *65* (34), 7146−7150.
(36) Saleh, S.; Picquet, M.; Meunier, P.; Hierso, J.-C. *Synlett* **2011**, *2011* (19), 2844−2848.
(37) Liang, B.; Dai, M.; Chen, J.; Yang, Z. *J. Org. Chem.* **2005**, *70* (1), 391−393.
(38) Gu, Z.; Li, Z.; Liu, Z.; Wang, Y.; Liu, C.; Xiang, J. *Catal. Commun.* **2008**, *9* (13), 2154−2157.
(39) Fukuyama, T.; Shinmen, M.; Nishitani, S.; Sato, M.; Ryu, I. *Org. Lett.* **2002**, *4* (10), 1691−1694.
(40) Shu, W.; Buchwald, S. L. *Chem. Sci.* **2011**, *2* (12), 2321.
(41) Torborg, C.; Beller, M. *Adv. Synth. Catal.* **2009**, *351* (18), 3027−3043.
(42) Torborg, C.; Huang, J.; Schulz, T.; Schäffner, B.; Zapf, A.; Spannenberg, A.; Börner, A.; Beller, M. *Chem. - Eur. J.* **2009**, *15* (6), 1329−1336.
(43) Hu, H.; Yang, F.; Wu, Y. *J. Org. Chem.* **2013**, *78* (20), 10506−10511.
(44) Yi, C.; Hua, R. *J. Org. Chem.* **2006**, *71* (6), 2535−2537.
(45) Yi, C.; Hua, R.; Zeng, H.; Huang, Q. *Adv. Synth. Catal.* **2007**, *349* (10), 1738−1742.
(46) Li, H.; Grasa, G. A.; Colacot, T. J. *Org. Lett.* **2010**, *12* (15), 3332−3335.
(47) Li, H.; Johansson Seechurn, C. C. C.; Colacot, T. J. *ACS Catal.* **2012**, *2* (6), 1147−1164.
(48) Fleckenstein, C. A.; Plenio, H. *Green Chem.* **2008**, *10* (5), 563.
(49) Yang, Y.; Chew, X.; Johannes, C. W.; Robins, E. G.; Jong, H.; Lim, Y. H. *Eur. J. Org. Chem.* **2014**, *2014* (32), 7184−7192.
(50) Yang, Y.; Lim, J. F. Y.; Chew, X.; Robins, E. G.; Johannes, C. W.; Lim, Y. H.; Jong, H. *Catal. Sci. Technol.* **2015**, *5* (7), 3501−3506.
(51) Tay, D. W.; Jong, H.; Lim, Y. H.; Wu, W.; Chew, X.; Robins, E. G.; Johannes, C. W. *J. Org. Chem.* **2015**, *80* (8), 4054−4063.
(52) Amatore, C.; Bensalem, S.; Ghalem, S.; Jutand, A.; Medjour, Y. *Eur. J. Org. Chem.* **2004**, *2004* (2), 366−371.
(53) Braga, A. A. C.; Ujaque, G.; Maseras, F. *Organometallics* **2006**, *25* (15), 3647−3658.
(54) Sikk, L.; Tammiku-Taul, J.; Burk, P. *Organometallics* **2011**, *30* (21), 5656−5664.
(55) García-Melchor, M.; Pacheco, M. C.; Nájera, C.; Lledós, A.; Ujaque, G. *ACS Catal.* **2012**, *2* (1), 135−144.
(56) Vikse, K. L.; Ahmadi, Z.; Manning, C. C.; Harrington, D. A.; McIndoe, J. S. *Angew. Chem., Int. Ed.* **2011**, *50* (36), 8304−8306.
(57) Sikk, L.; Tammiku-Taul, J.; Burk, P. *Proc. Est. Acad. Sci.* **2013**, *62* (2), 133.
(58) Bonney, K. J.; Schoenebeck, F. *Chem. Soc. Rev.* **2014**, *43* (18), 6609.
(59) Sperger, T.; Sanhueza, I. A.; Kalvet, I.; Schoenebeck, F. *Chem. Rev.* **2015**, *115* (17), 9532−9586.
(60) Maimone, T. J.; Milner, P. J.; Kinzel, T.; Zhang, Y.; Takase, M. K.; Buchwald, S. L. *J. Am. Chem. Soc.* **2011**, *133* (45), 18106−18109.
(61) Milner, P. J.; Maimone, T. J.; Su, M.; Chen, J.; Müller, P.; Buchwald, S. L. *J. Am. Chem. Soc.* **2012**, *134* (48), 19922−19934.
(62) Casado, A. L.; Espinet, P. *Organometallics* **1998**, *17* (5), 954−959.
(63) Dieck, H. A.; Heck, F. R. *J. Organomet. Chem.* **1975**, *93* (2), 259−263.
(64) Ljungdahl, T.; Bennur, T.; Dallas, A.; Emtenäs, H.; Mårtensson, J. *Organometallics* **2008**, *27* (11), 2490−2498.
(65) Perdew, J. P.; Burke, K.; Ernzerhof, M. *Phys. Rev. Lett.* **1996**, *77* (18), 3865−3868.
(66) Hay, P. J.; Wadt, W. R. *J. Chem. Phys.* **1985**, *82* (1), 270.
(67) Hay, P. J.; Wadt, W. R. *J. Chem. Phys.* **1985**, *82* (1), 299.
(68) Wadt, W. R.; Hay, P. J. *J. Chem. Phys.* **1985**, *82* (1), 284.
(69) Shao, Y.; Gan, Z.; Epifanovsky, E.; Gilbert, A. T. B.; Wormit, M.; Kussmann, J.; Lange, A. W.; Behn, A.; Deng, J.; Feng, X.; Ghosh, D.;

DOI: 10.1021/acs.organomet.6b00186
Organometallics XXXX, XXX, XXX−XXX

Goldey, M.; Horn, P. R.; Jacobson, L. D.; Kaliman, I.; Khaliullin, R. Z.; Kuś, T.; Landau, A.; Liu, J.; Proynov, E. I.; Rhee, Y. M.; Richard, R. M.; Rohrdanz, M. A.; Steele, R. P.; Sundstrom, E. J.; Woodcock, H. L.; Zimmerman, P. M.; Zuev, D.; Albrecht, B.; Alguire, E.; Austin, B.; Beran, G. J. O.; Bernard, Y. A.; Berquist, E.; Brandhorst, K.; Bravaya, K. B.; Brown, S. T.; Casanova, D.; Chang, C.-M.; Chen, Y.; Chien, S. H.; Closser, K. D.; Crittenden, D. L.; Diedenhofen, M.; DiStasio, R. A.; Do, H.; Dutoi, A. D.; Edgar, R. G.; Fatehi, S.; Fusti-Molnar, L.; Ghysels, A.; Golubeva-Zadorozhnaya, A.; Gomes, J.; Hanson-Heine, M. W. D.; Harbach, P. H. P.; Hauser, A. W.; Hohenstein, E. G.; Holden, Z. C.; Jagau, T.-C.; Ji, H.; Kaduk, B.; Khistyaev, K.; Kim, J.; Kim, J.; King, R. A.; Klunzinger, P.; Kosenkov, D.; Kowalczyk, T.; Krauter, C. M.; Lao, K. U.; Laurent, A. D.; Lawler, K. V.; Levchenko, S. V.; Lin, C. Y.; Liu, F.; Livshits, E.; Lochan, R. C.; Luenser, A.; Manohar, P.; Manzer, S. F.; Mao, S.-P.; Mardirossian, N.; Marenich, A. V.; Maurer, S. A.; Mayhall, N. J.; Neuscamman, E.; Oana, C. M.; Olivares-Amaya, R.; O'Neill, D. P.; Parkhill, J. A.; Perrine, T. M.; Peverati, R.; Prociuk, A.; Rehn, D. R.; Rosta, E.; Russ, N. J.; Sharada, S. M.; Sharma, S.; Small, D. W.; Sodt, A.; Stein, T.; Stück, D.; Su, Y.-C.; Thom, A. J. W.; Tsuchimochi, T.; Vanovschi, V.; Vogt, L.; Vydrov, O.; Wang, T.; Watson, M. A.; Wenzel, J.; White, A.; Williams, C. F.; Yang, J.; Yeganeh, S.; Yost, S. R.; You, Z.-Q.; Zhang, I. Y.; Zhang, X.; Zhao, Y.; Brooks, B. R.; Chan, G. K. L.; Chipman, D. M.; Cramer, C. J.; Goddard, W. A.; Gordon, M. S.; Hehre, W. J.; Klamt, A.; Schaefer, H. F.; Schmidt, M. W.; Sherrill, C. D.; Truhlar, D. G.; Warshel, A.; Xu, X.; Aspuru-Guzik, A.; Baer, R.; Bell, A. T.; Besley, N. A.; Chai, J.-D.; Dreuw, A.; Dunietz, B. D.; Furlani, T. R.; Gwaltney, S. R.; Hsu, C.-P.; Jung, Y.; Kong, J.; Lambrecht, D. S.; Liang, W.; Ochsenfeld, C.; Rassolov, V. A.; Slipchenko, L. V.; Subotnik, J. E.; Van Voorhis, T.; Herbert, J. M.; Krylov, A. I.; Gill, P. M. W.; Head-Gordon, M. *Mol. Phys.* **2015**, *113* (2), 184−215.

(70) Fukui, K. *Acc. Chem. Res.* **1981**, *14* (12), 363−368.

(71) Fauvarque, J.-F.; Pflüger, F.; Troupel, M. *J. Organomet. Chem.* **1981**, *208* (3), 419−427.

(72) Dai, C.; Fu, G. C. *J. Am. Chem. Soc.* **2001**, *123* (12), 2719−2724.

(73) Vikse, K.; Naka, T.; McIndoe, J. S.; Besora, M.; Maseras, F. *ChemCatChem* **2013**, *5* (12), 3604−3609.

(74) Fitton, P.; Rick, E. A. *J. Organomet. Chem.* **1971**, *28* (2), 287−291.

(75) Chatt, J.; Duncanson, L. A. *J. Chem. Soc.* **1953**, 2939.

(76) Matthews, W. S.; Bares, J. E.; Bartmess, J. E.; Bordwell, F. G.; Cornforth, F. J.; Drucker, G. E.; Margolin, Z.; McCallum, R. J.; McCollum, G. J.; Vanier, N. R. *J. Am. Chem. Soc.* **1975**, *97* (24), 7006−7014.

(77) Herrero, M. T.; de Sarralde, J. D.; SanMartin, R.; Bravo, L.; Domínguez, E. *Adv. Synth. Catal.* **2012**, *354* (16), 3054−3064.

(78) He, G.-W.; Liu, F.-W.; Xu, X.-H. *Chin. J. Org. Chem.* **2007**, *27* (5), 663−665.

(79) Zhang, Y.; Yu, D. Carboxylation of terminal alkynes. US Patent 20120323038A1, **2012**.

(80) Spitz, C.; Lohier, J.-F.; Reboul, V.; Metzner, P. *Org. Lett.* **2009**, *11* (13), 2776−2779.

DOI: 10.1021/acs.organomet.6b00186
Organometallics XXXX, XXX, XXX−XXX